Modeling of Correlated Stochastic Processes for the Transient Stability Analysis of Power Systems

Muhammad Adeen, *Student Member, IEEE*, Federico Milano, *Fellow, IEEE*

***Abstract*— This paper proposes a systematic and general approach to model correlated stochastic processes in power systems by means of stochastic differential-algebraic equations. The paper discusses the theoretical background of stochastic differential-algebraic equations and provides a variety of examples of correlated stochastic models for power system applications. With this aim, stochastic processes with Normal and Weibull distributions are considered. The case study utilizes the well-known two-area system to demonstrate that the presence of correlation between the stochastic processes can cause instability, despite the fact that the same system is stable if the same processes are uncorrelated. The case study also considers a 1479-bus dynamic model of the all-island Irish transmission system to show the scalability of the proposed technique, and to compare scenarios with different levels of correlation among stochastic processes. Results indicate that correlation has a non-negligible impact on short-term dynamics. A high level of correlation among the proecesses, in fact, can give raise to instability.**

***Index Terms*— Correlation, stochastic differential algebraic equations (SDAE), power system dynamics, time domain integration, Wiener process, Ornstein-Uhlenbeck process.**

I. Introduction

A. Motivation

Random fluctuations can be modeled as a set of stochastic processes, in the form of stochastic differential-algebraic equations (SDAEs) [1]–[3]. While in some cases such processes are local and independent, there exist processes that are intrinsically correlated. For example, in most locations, cloudy days tend to be more windy than clear-sky ones. Then the variations of the active and reactive power consumption of loads are coupled if the loads have a constant power factor. While the correlation of stochastic processes has been thoroughly discussed for unit-commitment and long-term power system operation problems, the impact of correlation among different stochastic processes on the short-term dynamics of power systems has not been discussed in the literature yet. This paper provides a general approach to model correlated processes by means of SDAEs and study the impact of such processes on power system dynamics.

B. Literature Review

Renewable energy resources such as wind and solar photovoltaic are non-dispatchable and are characterized by two kinds of stochastic behaviors: local fluctuations around a given average value; and uncertainty, which is related to operation and deviations with respect to forecasted values [4]. Loads power consumption are also not fully deterministic and are characterized by short- and long-term stochastic processes similar to renewable energy resources [5]. All these elements are responsible of introducing stochastic disturbances in the power systems. In this paper, we are interested in the short-term effects of noise, i.e. perturbations that are in the same time scale as voltage and angle transient stability analysis. This kind of noise is commonly known as "volatility."

A well-assessed technique that allows taking into account volatility in transient stability analysis is through a probabilistic analysis. Probabilistic analysis consists in initializing the set of differential-algebraic equations that model the system using a random initial value, chosen with given probability distributions [6]–[8]. The use of correlation in probabilistic analysis has been widely studied in recent years. In [9], the authors demonstrate that the risk assessment of line overload is highly affected by the spatial and temporal correlation between different wind speeds, and between power generation and load power consumption. In [10], the authors establish that the load forecast accuracy is dramatically improved if the correlation among load power consumption of different feeders is considered. In [11], the authors explain that the standard deviation of the output variables is underestimated if correlation among wind speeds at different wind farms, and load power consumption between different buses is not modeled properly. In [12], the authors demonstrate that the security-constrained unit commitment problem produces less conservative results if the uncertainty on the load power consumption and on wind speed is modeled by properly considering the correlation.

From the references above, it appears that the probabilistic analysis is particularly suited to study uncertainty. In dynamic studies based on probabilistic analysis, however, randomness is included only at the initial point, whereas the remainder of the simulation is deterministic. This can be useful to study the sensitivity of the model with respect to parameter uncertainty but, cannot take into account the dynamic behavior of stochastic processes.

For this reason, the impact of volatility on the dynamic response of power systems is better studied using stochastic differential-algebraic equations (SDAEs). This has been thoroughly explained in [1]–[3]. The latter reference also presents a general approach to incorporate stochastic processes in power systems using SDAEs. Some studies in the literature, i.e. [13]–[15], model power systems subject to stochastic disturbances as a set of stochastic differential equations (SDEs) not SDAEs and present stability indices to asses the small

The authors are with the School of Electrical and Electronic Engineering, University College Dublin, Ireland. (e-mails: muhammad.adeen@ucdconnect.ie and federico.milano@ucd.ie).

This work is supported by the Science Foundation Ireland, by funding Muhammad Adeen and Federico Milano under Investigator Programme Grant No. SFI/15/IA/3074.

signal stability and transient stability of power systems subject to uncertainty and volatility. In [16] the authors devise a method to determine the probability distribution of the power system frequency subject to stochastic load variations, and to evaluate the impact of different input parameters on the standard deviation of the frequency.

A common assumption of the literature available on SDEs or SDAEs models for power systems is that stochastic processes are fully uncorrelated. However, this is not always true. For example, the voltage on one side of a line/transformer is correlated to the voltage on the other side of that line/transformer. Similarly, there exists a correlation between the active and reactive load power consumption at a given bus. This aspect has been recently studied in [17] although this work only considers the correlation of two stochastic processes.

C. Contributions

To the best of our knowledge, this is the first work that discusses a systematic approach to study the effect of correlated stochastic processes on the transient behavior of power systems. The specific contributions of the paper are as follows.

- A general technique to model correlated stochastic processes with any probability distribution in power system models using large sets of nonlinear SDAEs.
- A procedure to set up correlated processes and quantify the effect of correlation among stochastic perturbations on the transient stability analysis of the power system.

It is important to note that the proposed model can be applied to systems of any order and complexity without the need of any simplifications or assumptions in the original model.

The manuscript shows that the correlation of stochastic processes plays a crucial role in the transient behavior of the system. In particular, we show that a certain set of processes with given probability distributions are harmless if they are fully uncorrelated but can drive the system to instability if correlated. This finding has a significant practical consequences, i.e., the need for system operators to take into account not only the probability distribution of the stochastic processes (such as wind and load power variations) but also the correlation among these processes.

D. Paper Organization

The remainder of the paper is organized as follows. Section II briefly outlines SDEs. The proposed approach to model correlated SDEs using correlated Wiener processes is presented in Section III. Section IV describes how to include correlated stochastic processes in power systems. Section V discusses realizations of correlated stationary stochastic processes, which follow different types of probability distributions, generated using correlated SDEs. Section VI presents a case study that discusses the impact of correlation of stochastic processes on the dynamic response of the two-area system, and the all-island Irish transmission system. Finally, Section VII draws conclusions and outlines future work.

II. Uncorrelated SDEs

A n-dimensional set of SDEs can be written as:

$$\dot{\boldsymbol{\kappa}}(t) = \boldsymbol{a}(\boldsymbol{\kappa}(t)) + \boldsymbol{b}(\boldsymbol{\kappa}(t)) \circ \boldsymbol{\xi}(t)\,, \tag{1}$$

where $\boldsymbol{a} : \mathbb{R}^n \mapsto \mathbb{R}^n)$ is a vector that represents the so called *drift* term, which is the deterministic part of an SDE and defines its long-term trend; $\boldsymbol{b} : \mathbb{R}^n \mapsto \mathbb{R}^n)$ is a vector that contains the *diffusion* term, which represents volatility, i.e. the amplitude of noise; $\boldsymbol{\xi}(t) \in \mathbb{R}^n$ is a vector of uncorrelated *Gaussian white noise*; and $\circ$ represents the Hadamard product, i.e. the element-wise product of two vectors. Mathematically, $\boldsymbol{\xi}(t)$ is defined as the time derivative of the Wiener process, as follows:

$$\boldsymbol{\xi}(t)\,dt = d\boldsymbol{W}(t)\,, \tag{2}$$

where $\boldsymbol{W} \in \mathbb{R}^{n_w}$ is a vector of standard uncorrelated Wiener process, whose elements, say $W_i(t)$, $i = 1, \ldots, n_w$, are fully independent and have the following properties:

1) $W_i(0) = 0$, with probability 1.
2) $W_i(t)$ is continuous for every t.
3) $W_i(t)$ has unbounded variation in every interval.
4) $W_i(t)$ has independent normal increments i.e., $\forall t \geq 0$, $dW_i = W_i(t+h) - W_i(t) \sim \mathcal{N}(0, h)$ where $\mathcal{N}(\mu, \sigma^2)$ represents the Normal distribution with mean μ and standard deviation σ.
5) $W_i(t)$ is non-differentiable for all t i.e., $\lim_{h\to 0}(W_i(t+h) - W_i(t))/h$ does not exist.

Note that the property 5 does not contradict the expression of the white noise given in (2), which is only a formal definition that allows to express SDEs in differential form but has no practical application. The integration of (1) only involves $d\boldsymbol{W}$ and sufficiently small time steps h [18]. In other words, $\boldsymbol{\xi}$ *per se* is not needed in the calculations and is never computed. In fact, substituting (2) into (1) and integrating the result one obtains the common integral form of SDEs, which is the one actually implemented in numerical tools:

$$\boldsymbol{\kappa}(t) = \int_t \boldsymbol{a}(\boldsymbol{\kappa}(\tau))\,d\tau + \int_W \boldsymbol{b}(\boldsymbol{\kappa}(\tau)) \circ d\boldsymbol{W}(\tau)\,. \tag{3}$$

Equation (1) can be solved by integrating its two terms, namely, drift and diffusion. The integration of the drift can be solved as a conventional Riemann-Stieltjes' integral. Any numerical method, such as the implicit trapezoidal method or the backward differentiation formulas can be utilized [19]. On the other hand, the integration of the diffusion term, which is associated to white noise, cannot be interpreted as an ordinary Riemann-Stieltjes' integral due to its stochastic nature. Several methods exist in the literature to interpret stochastic integral. Itô integral is the most popular choice in power systems. Since an analytical solution to an Itô SDE is not trivial or might not be available, numerical methods are usually employed. The Euler-Maruyama method is the most used to solve Itô SDEs by time discretization [20], [21].

III. Correlated SDEs

A. SDEs with Correlated Wiener Processes

Let us consider again the set of multi-dimensional SDEs defined in (1). These are uncorrelated if $\boldsymbol{W}$ is a vector of

independent Wiener processes. The elements of the covariance matrix $\mathbf{P} \in \mathbb{R}^{n\times n}$ of the increments $d\boldsymbol{W}$ are defined as follows:

$$P_{i,j} = \operatorname{cov}[dW_i, dW_j] = \begin{cases} \sigma_i^2, & \text{if } i = j\,, \\ 0, & \text{if } i \neq j\,, \end{cases} \tag{4}$$

We aim at constructing a vector of correlated Wiener processes. Suppose $\boldsymbol{V}$ is a vector of n elements that are obtained as the linear combination of the n uncorrelated Wiener processes $\boldsymbol{W}$. The correlation matrix $\mathbf{R} \in \mathbb{R}^{n\times n}$ for $\boldsymbol{V}$ has the form:

$$\mathbf{R} = \begin{bmatrix} 1 & r_{1,2} & r_{1,3} & \dots & r_{1,n} \\ r_{2,1} & 1 & r_{2,3} & \dots & r_{2,n} \\ r_{3,1} & r_{3,2} & 1 & \dots & r_{3,n} \\ \vdots & \vdots & \vdots & \ddots & \vdots \\ r_{n,1} & r_{n,2} & r_{n,3} & \cdots & 1 \end{bmatrix},$$

where $r_{i,j} = \operatorname{corr}[dV_i, dV_j]$ represents the correlation between dV_i and dV_j. Of course, $r_{i,j} = 1$ if $i = j$, since the correlation of any variable with itself is always 1.

The value of r can be calculated using the Pearson's correlation coefficient [22]. The elements of covariance matrix $\mathbf{P} \in \mathbb{R}^{n\times n}$ of $d\boldsymbol{V}$ are written as:

$$P_{i,j} = \operatorname{cov}[dV_i, dV_j] = \begin{cases} \sigma_i^2, & \text{if } i = j\,, \\ r_{i,j}\sigma_i\sigma_j, & \text{if } i \neq j\,, \end{cases} \tag{5}$$

The correlation between two processes can be considered either a constant or a stationary stochastic process during the period of simulation. The latter is defined using (1) as:

$$\dot{r}(t) = a(r(t)) + b(r(t))\xi(t)\,, \tag{6}$$

The technique explained in this paper is equally applicable to the case of correlation being a stochastic process, as the value of correlation is just a entry in the correlation matrix $\mathbf{R}$, which can be updated from the process (6) at every time step during the integration process.

The procedure to write $d\boldsymbol{V}$ in terms of $d\boldsymbol{W}$ is involved and is thoroughly explained in [23]. Here, we simply provide the final expression:

$$d\boldsymbol{V} = \mathbf{C}\, d\boldsymbol{W}\,, \tag{7}$$

where $\mathbf{C} \in \mathbb{R}^{n\times n}$ is chosen such that:

$$\mathbf{R} = \mathbf{C}\,\mathbf{C}^T\,. \tag{8}$$

A family of $\mathbf{C}$ matrices satisfies (8) but the best choice of $\mathbf{C}$ is a lower triangular matrix as it reduces memory requirements and the computational burden of numerical implementations. A lower triangular matrix is obtained by performing Cholesky-decomposition of $\mathbf{R}$. Cholesky-decomposition requires that the input matrix is positive semi-definite. This condition is generally satisfied for stochastic processes of power systems.

Based on the definitions above, a n-dimensional correlated SDE is constructed by substituting (7) into (1) as follows:

$$\begin{aligned} \dot{\boldsymbol{\eta}}(t) &= \boldsymbol{a}(\boldsymbol{\eta}(t)) + \boldsymbol{b}(\boldsymbol{\eta}(t)) \circ \boldsymbol{\zeta}(t)\,, \\ \boldsymbol{\zeta}(t) &= \mathbf{C}\,\boldsymbol{\xi}(t)\,, \end{aligned} \tag{9}$$

where $\boldsymbol{a}$, $\boldsymbol{b}$ and $\boldsymbol{\xi}$ have the same meaning as in (1); $\mathbf{C}$ satisfies (8); $\boldsymbol{\eta} \in \mathbb{R}^n$ is the vector of correlated stochastic processes; and $\boldsymbol{\zeta} \in \mathbb{R}^n$ is the vector of correlated white noises.

B. Special Case of Two-dimensional Correlated SDE

This section discusses a relevant special case of (9), namely a two-dimensional correlated stochastic process, which is helpful, for example, to model correlated active and reactive load power consumption. The correlation matrix $\mathbf{R}$ for a two-dimensional case is:

$$\mathbf{R} = \begin{bmatrix} 1 & r \\ r & 1 \end{bmatrix},$$

where r is Pearson correlation coefficient between the two processes. The Cholesky-decomposition of $\mathbf{R}$ gives $\mathbf{C}$ as:

$$\mathbf{C} = \begin{bmatrix} 1 & 0 \\ r & \sqrt{1-r^2} \end{bmatrix}.$$

From (9), a two-dimensional correlated SDE can be written as:

$$\begin{aligned} \dot{\eta}_1(t) &= a_1(\eta_1(t)) + b_1(\eta_1(t))\,\xi_1(t)\,, \\ \dot{\eta}_2(t) &= a_2(\eta_2(t)) + b_2(\eta_2(t))\big(r\,\xi_1(t) + \sqrt{1-r^2}\,\xi_2(t)\big)\,. \end{aligned} \tag{10}$$

IV. Modeling Volatility in Power Systems

As discussed in the introduction, the sources of volatility in power systems are the stochastic perturbations originated from physical processes such as stochastic load consumption, unbalanced conditions and harmonics that distort bus voltage phasors, and wind speed fluctuations.

Conventional dynamic stochastic models of power systems consider fully uncorrelated processes as in (1). When including such processes into the power system model, one obtains:

$$\begin{aligned} \dot{\boldsymbol{x}}(t) &= \boldsymbol{f}(\boldsymbol{x}(t), \boldsymbol{y}(t), \boldsymbol{\kappa}(t), \boldsymbol{u}(t))\,, \\ \mathbf{0} &= \boldsymbol{g}(\boldsymbol{x}(t), \boldsymbol{y}(t), \boldsymbol{\kappa}(t), \boldsymbol{u}(t))\,, \\ \dot{\boldsymbol{\kappa}}(t) &= \boldsymbol{a}(\boldsymbol{\kappa}(t)) + \boldsymbol{b}(\boldsymbol{\kappa}(t)) \circ \boldsymbol{\xi}(t)\,, \end{aligned} \tag{11}$$

where $\boldsymbol{x} \in \mathbb{R}^m$ is a vector of state variables; $\boldsymbol{y} \in \mathbb{R}^l$ is a vector of algebraic variables; $\boldsymbol{u} \in \mathbb{R}^s$ is a vector of discrete variables; $\boldsymbol{f} : \mathbb{R}^{m+l+n+s} \mapsto \mathbb{R}^m$ are the differential equations; $\boldsymbol{g} : \mathbb{R}^{m+l+n+s} \mapsto \mathbb{R}^l$ are the algebraic equations; and $\dot{\boldsymbol{\kappa}}$ are defined as in (1). The set of SDAEs in (11) is the model that was proposed in [3] and several other reference thereinafter.

Elaborating on (11) and (9), the set of SDAEs that describes a power system model with inclusion of n correlated processes can be thus written as follows:

$$\begin{aligned} \dot{\boldsymbol{x}}(t) &= \boldsymbol{f}(\boldsymbol{x}(t), \boldsymbol{y}(t), \boldsymbol{\eta}(t), \boldsymbol{u}(t))\,, \\ \mathbf{0} &= \boldsymbol{g}(\boldsymbol{x}(t), \boldsymbol{y}(t), \boldsymbol{\eta}(t), \boldsymbol{u}(t))\,, \\ \dot{\boldsymbol{\eta}}(t) &= \boldsymbol{a}(\boldsymbol{\eta}(t)) + \boldsymbol{b}(\boldsymbol{\eta}(t)) \circ [\mathbf{C}\,\boldsymbol{\xi}(t)]\,. \end{aligned} \tag{12}$$

Note that numerical algorithms, to generate random numbers, can be utilized to generate independent Wiener processes and thus $\boldsymbol{\zeta}$ can be obtained only indirectly, i.e. through the calculation of $\mathbf{C}\,\boldsymbol{\xi}$.

A. Stochastic Load Model

Stochastic load models are well-established in the literature [24]. The stochastic load model introduced in [3] considers the well-known voltage dependent load model and uses uncorrelated OUPs to define volatility on active and reactive load power consumption. This is the starting point of the models presented in this paper.

1) Correlated Active and Reactive Power Consumption: The two-dimensional correlated SDEs introduced in Section III-B are used to model correlated volatility on active and reactive load power consumption. The proposed model is as follows:

$$\begin{aligned} p_{\mathrm{L}}(t) &= (p_{\mathrm{L0}} + \eta_p(t))(v(t)/v_0)^{\gamma_p}\,, \\ q_{\mathrm{L}}(t) &= (q_{\mathrm{L0}} + \eta_q(t))(v(t)/v_0)^{\gamma_q}\,, \\ \dot{\eta}_p(t) &= a_p(\eta_p(t)) + b_p(\eta_p(t))\,\xi_p(t)\,, \\ \dot{\eta}_q(t) &= a_q(\eta_q(t)) + b_q(\eta_q(t))(r_{p,q}\,\xi_p(t) + \sqrt{1-r_{p,q}^2}\,\xi_q(t))\,, \end{aligned} \tag{13}$$

where p_{L0} and q_{L0} are the nominal values of active and reactive power consumption, respectively; $v(t)$ represents the magnitude of the bus voltage at the load bus; v_0 is the initial value of this voltage magnitude at time $t = 0$; and γ_p and γ_q impose the voltage dependency of the load, i.e., $\gamma_p = \gamma_q = 0$ is for constant power and $\gamma_p = \gamma_q = 2$ for constant impedance loads.

In (13), the volatility on active and reactive power consumption is modeled through two-dimensional correlated SDEs, and parameters a and b have the same meaning as in (10). Parameter $r_{p,q}$ represents the correlation between the two processes, i.e. η_p and η_q. Note that a value of $r_{p,q} = 0$ means that the volatility on the active and reactive power consumption is uncorrelated, thus, leading to the load model in [3].

2) Correlation on Load Power Consumption between Different Load Buses: In practice, some level of spatial and temporal correlation exists between load power consumption at different load buses. This is true because consumer behavior is correlated. This behavior is represented by correlated volatility and is modeled using n-dimensional correlated SDEs. The model in (13) is thus modified to include the correlation between the load consumption of d buses:

$$\begin{aligned} \boldsymbol{p}_{\mathrm{L}}(t) &= (\boldsymbol{p}_{\mathrm{L0}} + \boldsymbol{\eta}_p(t)) \circ \boldsymbol{v}_p(t)\,, \\ \boldsymbol{q}_{\mathrm{L}}(t) &= (\boldsymbol{q}_{\mathrm{L0}} + \boldsymbol{\eta}_q(t)) \circ \boldsymbol{v}_q(t)\,, \\ \begin{bmatrix} \dot{\boldsymbol{\eta}}_p(t) \\ \dot{\boldsymbol{\eta}}_q(t) \end{bmatrix} &= \begin{bmatrix} \boldsymbol{a}_p(\boldsymbol{\eta}_p(t)) \\ \boldsymbol{a}_q(\boldsymbol{\eta}_q(t)) \end{bmatrix} + \begin{bmatrix} \boldsymbol{b}_p(\boldsymbol{\eta}_p(t)) \\ \boldsymbol{b}_q(\boldsymbol{\eta}_q(t)) \end{bmatrix} \circ \mathbf{C} \begin{bmatrix} \boldsymbol{\xi}_p(t) \\ \boldsymbol{\xi}_q(t) \end{bmatrix}, \end{aligned} \tag{14}$$

where $\boldsymbol{p}_{\mathrm{L}} \in \mathbb{R}^d$ and $\boldsymbol{q}_{\mathrm{L}} \in \mathbb{R}^d$ represent the active and reactive power consumption at load buses, respectively; $\boldsymbol{p}_{\mathrm{L0}} \in \mathbb{R}^d$ and $\boldsymbol{q}_{\mathrm{L0}} \in \mathbb{R}^d$ represent the nominal active and nominal reactive power consumption at load buses, respectively; $\boldsymbol{v}_p \in \mathbb{R}^d$ and $\boldsymbol{v}_q \in \mathbb{R}^d$ represent vectors whose elements are calculated as:

$$\begin{aligned} v_{p,i}(t) &= (v_i(t)/v_{0,i})^{\gamma_{p,i}}\,, \quad i = 1, \ldots, d\,, \\ v_{q,i}(t) &= (v_i(t)/v_{0,i})^{\gamma_{q,i}}\,, \quad i = 1, \ldots, d\,, \end{aligned}$$

respectively; and $\boldsymbol{a}_p$, $\boldsymbol{a}_q$, $\boldsymbol{b}_p$ and $\boldsymbol{b}_q$ are all d-dimensional vectors with same meanings as in (9). Matrix $\mathbf{C} \in \mathbb{R}^{2d \times 2d}$ and is obtained as the Cholesky decomposition of a correlation matrix $\mathbf{R}$ with the following structure:

$$\mathbf{R} = \begin{bmatrix} \mathbf{R}_{p,p} & \mathbf{R}_{p,q} \\ \mathbf{R}_{q,p} & \mathbf{R}_{q,q} \end{bmatrix}, \tag{15}$$

where $\mathbf{R}_{q,p} = \mathbf{R}_{p,q}^T$ and:

$$\mathbf{R}_{p,p} = \begin{bmatrix} 1 & r_{p_1,p_2} & \cdots & r_{p_1,p_d} \\ r_{p_2,p_1} & 1 & \cdots & r_{p_2,p_d} \\ \vdots & \vdots & \ddots & \vdots \\ r_{p_d,p_1} & r_{p_d,p_2} & \cdots & 1 \end{bmatrix},$$

$$\mathbf{R}_{p,q} = \begin{bmatrix} r_{p_1,q_1} & r_{p_1,q_2} & \cdots & r_{p_1,q_d} \\ r_{p_2,q_1} & r_{p_2,q_2} & \cdots & r_{p_2,q_d} \\ \vdots & \vdots & \ddots & \vdots \\ r_{p_d,q_1} & r_{p_d,q_2} & \cdots & r_{p_d,q_d} \end{bmatrix},$$

$$\mathbf{R}_{q,q} = \begin{bmatrix} 1 & r_{q_1,q_2} & \cdots & r_{q_1,q_d} \\ r_{q_2,q_1} & 1 & \cdots & r_{q_2,q_d} \\ \vdots & \vdots & \ddots & \vdots \\ r_{q_d,q_1} & r_{q_d,q_2} & \cdots & 1 \end{bmatrix}.$$

B. Stochastic Power Flow Equations

To ensure a secure operation of the grid, it is required that generation and demand are balanced at all times. The power balance at i-th bus is given by the well-known power flow equations, which in polar form are written as:

$$\begin{aligned} 0 &= p_{\mathrm{G},i}(t) - p_{\mathrm{L},i}(t) \\ &\quad - \hat{v}_i(t) \sum_{j=1}^{n_{\mathrm{B}}} [\hat{v}_j(t) B_{ij} \sin(\hat{\theta}_i(t) - \hat{\theta}_j(t)) \\ &\quad + \hat{v}_i(t) G_{ij} \cos(\hat{\theta}_i(t) - \hat{\theta}_j(t))]\,, \quad i = 1, \ldots, n_{\mathrm{B}}\,, \\ 0 &= q_{\mathrm{G},i}(t) - q_{\mathrm{L},i}(t) \\ &\quad - \hat{v}_i(t) \sum_{j=1}^{n_{\mathrm{B}}} [\hat{v}_j G_{ij} \sin(\hat{\theta}_i(t) - \hat{\theta}_j(t)) \\ &\quad - \hat{v}_j(t) B_{ij} \cos(\hat{\theta}_i(t) - \hat{\theta}_j(t))]\,, \quad i = 1, \ldots, n_{\mathrm{B}}\,, \end{aligned} \tag{16}$$

where $p_{\mathrm{G},i}$ and $q_{\mathrm{G},i}$ represent the sum of the active power generation, and the sum of reactive power generation at the i-th bus, respectively. Similarly, $p_{\mathrm{L},i}$ and $q_{\mathrm{L},i}$ is the sum of the active power consumption, and the sum of the reactive power consumption at the i-th bus, respectively. n_{B} is the total number of buses of the grid. G_{ij} and B_{ij}, respectively, are the real and imaginary part of the (i, j) element of the system admittance matrix.

In [3], noise is included in the bus voltage phasor to account for possible sources of volatility and fluctuations not modelled in the set of DAEs for transient stability analysis, e.g., the effects of harmonics, nonlinearities, load unbalances, and electromagnetic transients, etc. In the same vein, the stochastic processes in (16) are included through the variables $\hat{v}_i$ and $\hat{\theta}_i$, which are the bus voltage magnitude and the voltage phase angle, respectively, and are obtained as n_{B}-dimensional correlated SDEs as follows:

$$\begin{aligned} \hat{\boldsymbol{v}}(t) &= \boldsymbol{v}(t) - \boldsymbol{\eta}_v(t)\,, \\ \hat{\boldsymbol{\theta}}(t) &= \boldsymbol{\theta}(t) - \boldsymbol{\eta}_\theta(t)\,, \\ \begin{bmatrix} \dot{\boldsymbol{\eta}}_v(t) \\ \dot{\boldsymbol{\eta}}_\theta(t) \end{bmatrix} &= \begin{bmatrix} \boldsymbol{a}_v(\boldsymbol{\eta}_v(t)) \\ \boldsymbol{a}_\theta(\boldsymbol{\eta}_\theta(t)) \end{bmatrix} + \begin{bmatrix} \boldsymbol{b}_v(\boldsymbol{\eta}_v(t)) \\ \boldsymbol{b}_\theta(\boldsymbol{\eta}_\theta(t)) \end{bmatrix} \circ \mathbf{C} \begin{bmatrix} \boldsymbol{\xi}_v(t) \\ \boldsymbol{\xi}_\theta(t) \end{bmatrix}, \end{aligned} \tag{17}$$

where $\boldsymbol{v} \in \mathbb{R}^{n_{\mathrm{B}}}$ and $\boldsymbol{\theta} \in \mathbb{R}^{n_{\mathrm{B}}}$ are the noise-free components of the voltage magnitude and phase angles, respectively, at

network buses; and $\boldsymbol{a}_v$, $\boldsymbol{a}_\theta$, $\boldsymbol{b}_v$ and $\boldsymbol{b}_\theta$ are all n_{B}-dimensional vectors with same meanings as in (9). $\mathbf{C} \in \mathbb{R}^{2n_{\mathrm{B}} \times 2n_{\mathrm{B}}}$ is calculated based on the correlation matrix, using (8), using a correlation matrix $\mathbf{R}$ that contains the correlation values between voltage magnitudes and voltage angles. The structure of $\mathbf{R}$ is similar to that of (15), namely:

$$\mathbf{R} = \begin{bmatrix} \mathbf{R}_{v,v} & \mathbf{R}_{v,\theta} \\ \mathbf{R}_{\theta,v} & \mathbf{R}_{\theta,\theta} \end{bmatrix}, \tag{18}$$

where $\mathbf{R}_{\theta,v} = \mathbf{R}_{v,\theta}^T$ and:

$$\mathbf{R}_{v,v} = \begin{bmatrix} 1 & r_{v_1,v_2} & \dots & r_{v_1,v_d} \\ r_{v_2,v_1} & 1 & \dots & r_{v_2,v_d} \\ \vdots & \vdots & \ddots & \vdots \\ r_{v_d,v_1} & r_{v_d,v_2} & \dots & 1 \end{bmatrix},$$

$$\mathbf{R}_{v,\theta} = \begin{bmatrix} r_{v_1,\theta_1} & r_{v_1,\theta_2} & \dots & r_{v_1,\theta_d} \\ r_{v_2,\theta_1} & r_{v_2,\theta_2} & \dots & r_{v_2,\theta_d} \\ \vdots & \vdots & \ddots & \vdots \\ r_{v_d,\theta_1} & r_{v_d,\theta_2} & \dots & r_{v_d,\theta_d} \end{bmatrix},$$

$$\mathbf{R}_{\theta,\theta} = \begin{bmatrix} 1 & r_{\theta_1,\theta_2} & \dots & r_{\theta_1,\theta_d} \\ r_{\theta_2,\theta_1} & 1 & \dots & r_{\theta_2,\theta_d} \\ \vdots & \vdots & \ddots & \vdots \\ r_{\theta_d,\theta_1} & r_{\theta_d,\theta_2} & \dots & 1 \end{bmatrix}.$$

C. Wind Fluctuations

The electrical power generated from wind farms is a function of the wind speed, which is highly affected by weather conditions. The wind speed is a physical process that exhibits volatility. Wind speed is modeled as a stochastic perturbation in power systems. Due to the stochastic nature of the wind speed, it becomes highly important to study its effects on power system dynamics to ensure a secure and reliable operation. The uncorrelated volatility model of wind speed is the following:

$$\begin{aligned} w(t) &= w_0 + \eta_w(t)\,, \\ \dot{\eta}_w(t) &= a_w(\eta_w(t)) + b_w(\eta_w(t))\,\xi_w(t)\,, \end{aligned} \tag{19}$$

where w_0 is the average wind speed in a given period, and the parameters a_w, and b_w, have the same meaning as in (1).

The spatial and temporal correlation between different wind turbines within a power plant, as well as among power plants can be modeled as a set of correlated wind speeds. Such a model is written as:

$$\begin{aligned} \boldsymbol{w}(t) &= \boldsymbol{w}_0 + \boldsymbol{\eta}_w(t)\,, \\ \dot{\boldsymbol{\eta}}_w(t) &= \boldsymbol{a}_w(\boldsymbol{\eta}_w(t)) + \boldsymbol{b}_w(\boldsymbol{\eta}_w(t)) \circ [\mathbf{C}\,\boldsymbol{\xi}_w(t)]\,. \end{aligned} \tag{20}$$

where $\boldsymbol{w}_0 \in \mathbb{R}^{n_{\mathrm{W}}}$ is the vector of uncorrelated wind speeds; $\mathbf{C} \in \mathbb{R}^{n_{\mathrm{W}} \times n_{\mathrm{W}}}$) is calculated from a wind correlation matrix $\mathbf{R}$ using (8); and other variables and parameters have same meaning as in (9).

V. Processes Generated Using Correlated SDEs

The correlated SDE introduced in (9) can be utilized to generate correlated stationary stochastic processes, which will follow any required probability density function, through the proper implementation of the drift a and diffusion b terms. In the examples and case study of this paper, we consider Normal and Weibull distributed stochastic processes. However, it is important to note that processes with any other probability distribution can be utilized. All types of distributions, in fact, can be created through the proper definition of a and b using the procedures described in [25]–[27].

A. Ornstein-Uhlenbeck process

The Ornstein-Uhlenbeck process (OUP) is a continuous stationary process with a normal probability density function. The OUP is widely utilized to model volatility in physical processes such as stochastic load dynamics [5], [28], [29] and wind fluctuations [30]–[32]. Correlated OUPs can be generated using (9) with the drift and diffusion term given as:

$$\begin{aligned} a(\eta(t)) &= -\alpha(\eta(t) - \mu)\,, \\ b(\eta(t)) &= \sqrt{2\alpha}\sigma\,, \end{aligned} \tag{21}$$

where α defines the auto-correlation coefficient of the process, μ is the mean value of the process at the stationary condition, σ is the standard deviation.

Figure 1 illustrates the realizations of two-dimensional correlated OUPs for different values of r while keeping α and σ constant. The probability densities of the OUPs in Figure 1 are shown in Figure 2. From Figure 2 it is evident that the processes η_1 and η_2 follow a Normal distribution, despite being generated for different values of r between them.

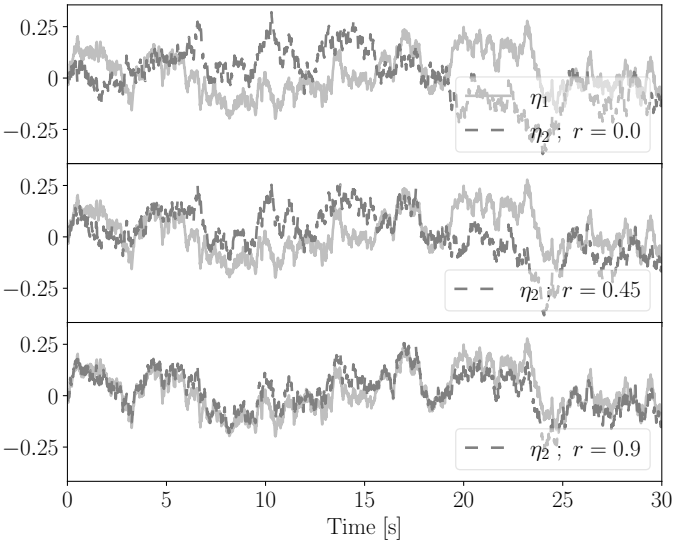

Fig. 1. Realizations of two-dimensional OUPs for different values of the correlation r, and for $\alpha_1 = \alpha_2 = 1s^{-1}$, and $\sigma_1 = \sigma_2 = 0.1$.

B. 2-Parameter Weibull Distributed Process

N-dimensional correlated Weibull distributed processes are generated using (9) with the drift term as:

$$a(\eta) = -\alpha\left(\eta - \lambda\Gamma\left(1 + \kappa^{-1}\right)\right), \tag{22}$$

and the diffusion term as:

$$b(\eta) = \sqrt{b_1(\eta) b_2(\eta)}\,, \tag{23}$$

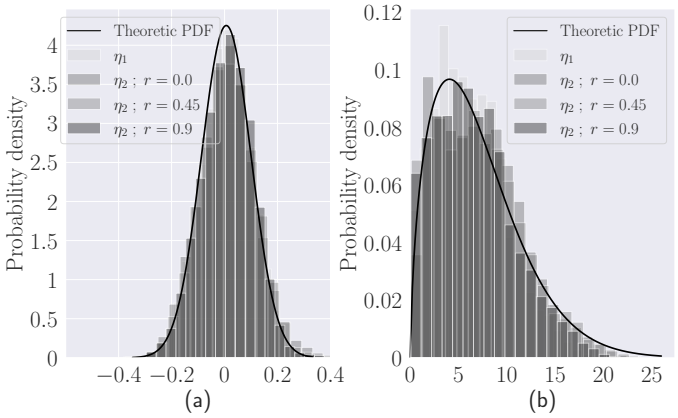

Fig. 2. (a) Probability distribution of OUP; and (b) Probability distribution of Weibull process, realized for different values of correlation.

with

$$b_1(\eta) = 2\alpha\,\eta\,c_1\frac{\lambda}{\kappa}\left(c_2\right)^{-\kappa}\,, \tag{24}$$

and

$$b_2(\eta) = \kappa\exp\left(\left(c_2\right)^{\kappa}\right)\Gamma\left(1+c_1,\left(c_2\right)^{\kappa}\right) - \Gamma\left(c_1\right) \tag{25}$$

where $c_1 = 1/\kappa$ and $c_2 = \eta/\lambda$; α is the autocorrelation coefficient; κ is a shape parameter; λ is a scale parameter; $\Gamma(\cdot)$ is the Gamma function; and $\Gamma(\cdot,\cdot)$ is the Incomplete Gamma function.

Figure 3 illustrates the realizations of two-dimensional correlated Weibull distributed processes for different values of r while keeping shape and scale constant. The probability densities of the Weibull distributed processes presented in Figure 3 are shown in Figure 2. This figure shows that the processes η_1 and η_2 follow, in effect, a Weibull distribution and can be correlated with each other while preserving their probability density annd other statistical properties.

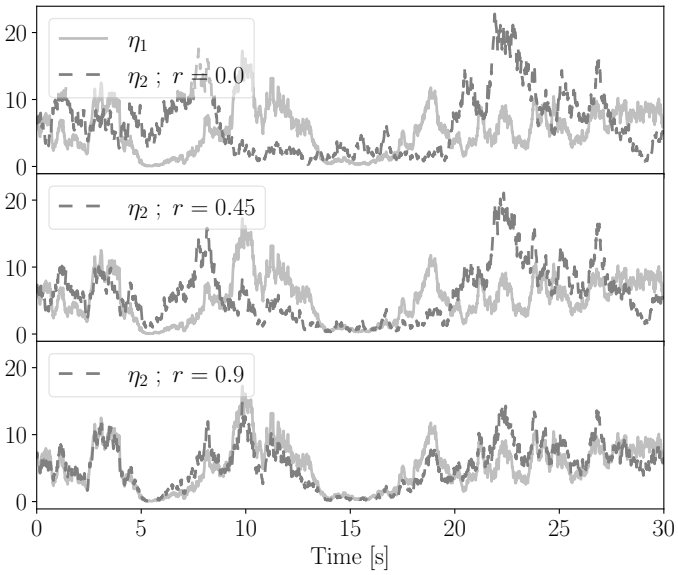

Fig. 3. Realizations of two-dimensional Weibull processes for different values of the correlation r, and for $\alpha_1 = \alpha_2 = 0.5s^{-1}$; $\lambda_1 = \lambda_2 = 8$; and $\kappa_1 = \kappa_2 = 2$.

VI. Case Study

This case study aims at evaluating the effect of the correlated stochastic processes on the dynamic behavior of power systems. With this goal, we compare the standard deviation of the trajectories of system variables such as the active power of synchronous generators and bus voltage magnitude considering the cases of correlated and uncorrelated stochastic processes. Two power systems are considered, namely, the well-known Kundur's two-area system, and a dynamic model of the All-Island Irish Transmission System (AIITS).

To study the impact of correlated stochastic perturbations on the electrical power system, we need first to define the correlation matrix $\mathbf{R}$. Data to account for the correlation among stochastic processes in the time scale of transient stability analysis are currently unavailable. Hence, we carry out a sensitivity analysis. With this aim, we define three scenarios S1, S2 and S3, as follows:

- S1 represents the fully uncorrelated SDAE model, i.e. the correlation between any two stochastic processes i and j is $r_{i,j} = 0$.
- S2 considers a low level of correlation among processes, i.e. the correlation between any two stochastic processes i and j is set to $r_{i,j} = 0.4$ if they belong to the same area, 0 otherwise.
- S3 considers a high level of correlation among processes, i.e. the value of correlation between any two stochastic processes i and j is set to $r_{i,j} = 0.8$ if they belong to the same area, 0 otherwise.

The loads are modeled as constant impedance loads. In this paper, we consider noise to be normally distributed. Other probability distributions can also be modeled using the procedures defined in Section V. The technique propsed in this paper, in fact, allows correlating stochastic processes independently from their probability distribution.

To evaluate the impact of the correlation of stochastic processes, we consider a Monte Carlo analysis and observe the trajectories of relevant quantities of the system. The Monte Carlo analysis consists in 1,000 time domain simulations per scenario. Each simulation requires about 8,000 realizations of the Wiener processes for all wind speeds, bus voltage phasors, and load active and reactive power consumption. The integration scheme utilizes a step size $h = 0.01$ s for the Maruyama-Euler integration of the Wiener processes and $\Delta t = 0.01$ s for the integration of the drift obtained with the implicit trapezoidal method.

The step size of 0.01 s is utilized in the simulations only to achieve accurate results. Larger sampling times, e.g., 0.1 s or 1 s, can be utilized to define the correlation of the stochastic processes. It is important to note that, while large amount of data are required to set up the correlation matrix, the technology to gather and store such data with the required sampling rate is already available. For example secondly measurements of wind were utilized in [33]; frequency measurements with a sampling time of 0.1 s were utilized in [34]; and power measurements with a sampling frequency of 120 Hz were utilized in [5]. It is also important to note that the measurements are required only to define the correlation

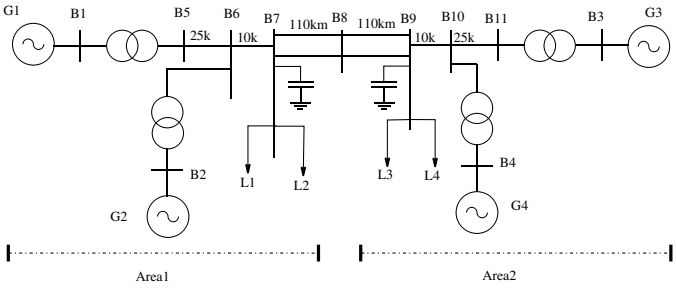

Fig. 4. Two-area system.

matrix and the probability distribution of the proecesses. After that, the model proposed in this paper is capable or generating synthetic noise with the same statistical properties and same correlation. The proposed approach, thus, does not need to be continuously fed with measurement data. This is, in turn, one of the practical advantages of the proposed method.

A. Two-Area System

The two-area system, shown in Fig. 4 and originally defined in [35], consists of 11 buses, 12 lines/transformers, and four synchronous generators, which are modeled via a 6th-order model and are equipped with IEEE ST1a exciters, turbine governors, and an AGC that coordinates the four synchronous generators.

Correlated stochastic processes are inclued into the two-area system through stochastic load consumption, and bus voltage phasors, with the following parameters: $\alpha_p = \alpha_q = \alpha_v = \alpha_\theta = 1\text{s}^{-1}$, $\sigma_p = 0.6\%$ of p_{L0}, $\sigma_q = 0.6\%$ of q_{L0}, $\sigma_v = 0.3\%$ of v_0 and $\sigma_\theta = 0.3\%$ of θ_0.

We first consider correlated volatility on load consumption, as discussed in Section IV-A.2. The correlation matrix utilized to model correlation on stochastic load consumption is shown in Table I, where the value of r represents the correlation between any two given quantities. The value of r is chosen based on the scenarios S1, S2, and S3. The paper considers correlation between the load devices connected in the same area. Hence, inter-area correlation is not considered. In this example, bus voltage phasors do not include noise. The trajectories of the voltage profile at bus 8 are observed for the three scenarios simulated, and the results are presented in Table II. Results indicate that the higher the correlation among processes, the higher the probability that the system becomes unstable. This result can be explained as follows: the loads will require more/less power from generators if they all increase/decrease in a coordinated manner. For illustration purposes, a selection of the unstable trajectories of voltage at bus 8 from scenarios S2, and S3, are shown in Figs. 5-6 and Figs. 7-8, respectively. Simulations indicate that the loss of stability, in this case, is due to a shortage of reactive power that leads to voltage collpase.

An effective way to evaluate the effect of correlation between the loads is through observing the statistical properties of the relevant quantities. The statistical property, and the quantity chosen in this case study is the standard deviation of the active and reactive power generation of synchronous

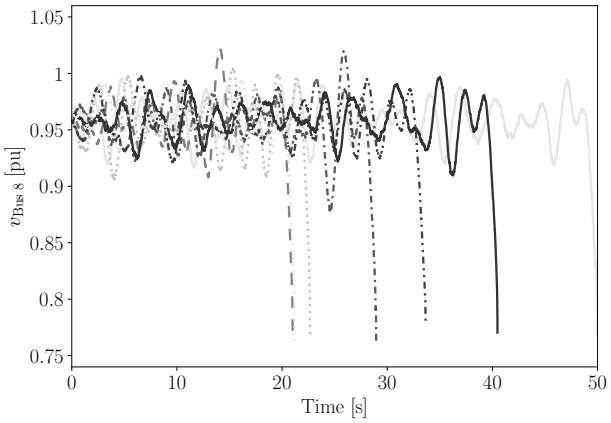

Fig. 5. Voltage profile at bus 8 of the two-area system for selected unstable trajectories for S2.

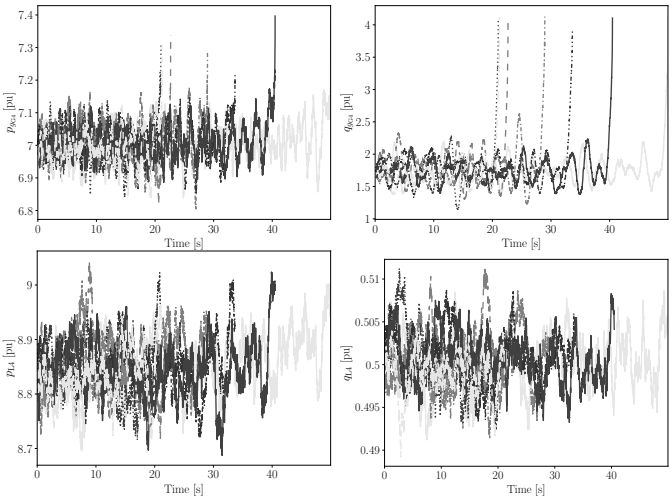

Fig. 6. Generator (upper panels) and load (lower panels) active (left panels) and reactive (right panels) power selected unstable trajectories for S2.

TABLE I

CORRELATION MATRIX OF THE LOADS OF THE TWO-AREA SYSTEM

	p_1	p_2	p_3	p_4	q_1	q_2	q_3	q_4
p_1	1	r	0	0	r	r	0	0
p_2	r	1	0	0	r	r	0	0
p_3	0	0	1	r	0	0	r	r
p_4	0	0	r	1	0	0	r	r
q_1	r	r	0	0	1	r	0	0
q_2	r	r	0	0	r	1	0	0
q_3	0	0	r	r	0	0	1	r
q_4	0	0	r	r	0	0	r	1

TABLE II

UNSTABLE TRAJECTORIES FOR THE TWO-AREA SYSTEM

Scenario	Unstable trajectories	Disconnection of load L_3: Unstable trajectories
S1	0	0
S2	68 (6.8%)	19 (1.9%)
S3	369 (36.9%)	68 (6.8%)

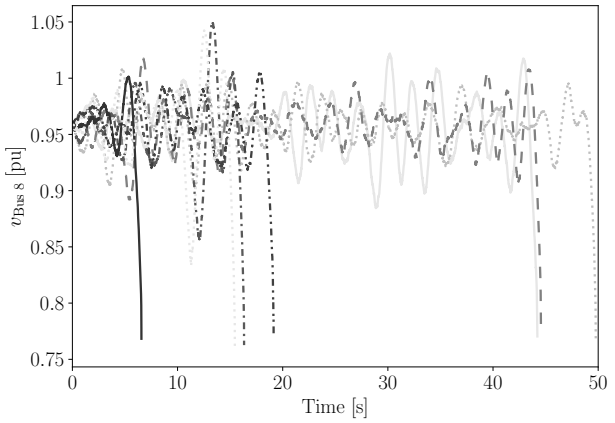

Fig. 7. Voltage profile at bus 8 of the two-area system for selected unstable trajectories for S3.

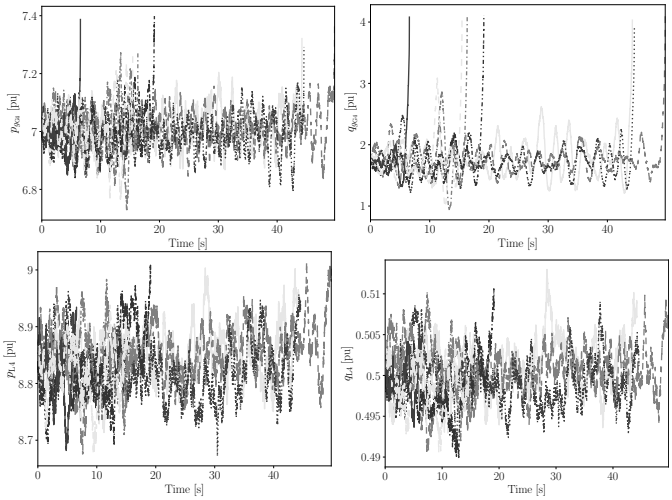

Fig. 8. Generator (upper panels) and load (lower panels) active (left panels) and reactive (right panels) power selected unstable trajectories for S3.

generators, namely, σ_{p_g} and σ_{q_g}, respectively. The standard deviation of stable trajectories of active p_g and reactive q_g power generation of synchronous generators obtained from the simulations presented above in this section is calculated and presented in Table III. This table indicates that the increase of the values of σ_{p_g} and σ_{q_g} increases by about 25% comparing scenarios S1 to S2 and by about 50% comparing scenarios S1 and S3.

Next, the impact of correlated noise of bus voltage phasors on σ_{p_g} and σ_{q_g} of the synchronous generators is evaluated by modeling the stochastic perturbations on the bus voltage phasors through correlated stochastic processes, as explained in Section IV-B. The correlation matrix is built in such a way that stochastic perturbations on every bus connected in the same area are considered to be correlated, whereas no correlation is considered between buses connected in different areas. In this example, load power consumption does not include noise. Table IV shows σ_{p_g} and σ_{q_g} of synchronous generators calculated for the three scenarios S1, S2, and S3. It appears that the correlation among the stochastic bus voltage phasors is inversely proportional to the σ_{p_g} and σ_{q_g} of the generators. Note that none of the trajectories were found to be unstable. This effect is thus the opposite as the one obtained when varying the correlation of the load power consumption.

TABLE III
STANDARD DEVIATION OF ACTIVE AND REACTIVE POWERS OF SYNCHRONOUS GENERATORS FOR THE TWO-AREA SYSTEM WITH CORRELATED STOCHASTIC LOADS

Standard deviation	S1 absolute	S2 % increase	S3 % increase
$p_{g_{\text{G1}}}$	0.0519	22.73	45.04
$p_{g_{\text{G2}}}$	0.0439	22.34	44.15
$p_{g_{\text{G3}}}$	0.0432	22.76	45.03
$p_{g_{\text{G4}}}$	0.0442	21.94	42.53
$q_{g_{\text{G1}}}$	0.1399	24.37	48.88
$q_{g_{\text{G2}}}$	0.1726	24.37	48.89
$q_{g_{\text{G3}}}$	0.1215	25.22	50.82
$q_{g_{\text{G4}}}$	0.1554	25.13	50.55

TABLE IV
STANDARD DEVIATION OF ACTIVE AND REACTIVE POWERS OF SYNCHRONOUS GENERATORS FOR THE TWO-AREA SYSTEM WITH CORRELATED STOCHASTIC VOLTAGES

Standard deviation	S1 absolute	S2 % increase	S3 % increase
$p_{g_{\text{G1}}}$	0.0495	-20.06	-47.24
$p_{g_{\text{G2}}}$	0.0547	-20.68	-49.20
$p_{g_{\text{G3}}}$	0.0908	-17.51	-39.67
$p_{g_{\text{G4}}}$	0.0909	-18.22	-41.70
$q_{g_{\text{G1}}}$	0.0598	-18.75	-42.93
$q_{g_{\text{G2}}}$	0.0705	-17.63	-40.22
$q_{g_{\text{G3}}}$	0.0420	-21.49	-50.79
$q_{g_{\text{G4}}}$	0.0516	-20.75	-49.49

Finally, we simulate the two-area system, shown in Figure 4, using correlated stochastic loads with the following parameters: $\alpha_p = \alpha_q = 1\text{s}^{-1}$, $\sigma_p = 0.5\%$ of p_{L0}, and $\sigma_q = 0.5\%$ of q_{L0}. Besides correlated stochastic loads, the system undergoes disconnection of load L_3 at $t = 10s$. The simulation results for unstable trajectories for the three scenarios of correlation are shown in Table II. The results show that the system experiences increased number of unstable trajectories for higher values of correlation. A few of such unstable trajectories of rotor angle δ of all the machines for scenario S2 are shown in Figure 9. Whereas, the stable trajectories of δ simulated for scenario S3 are shwon in Figure 10.

B. All-Island Irish Transmission System

AIITS consists of 1479 buses, 1851 lines/transformers, and 22 synchronous generators that are modeled through a VI-order model and are equipped with IEEE ST1a exciters and turbine governors to ensure a secure operation of the grid. 6 conventional power plants also include a power system stabilizer. The model also includes 176 wind power plants, 34 of which are equipped with constant-speed and 142 with doubly-fed induction generators. In this case study, we model

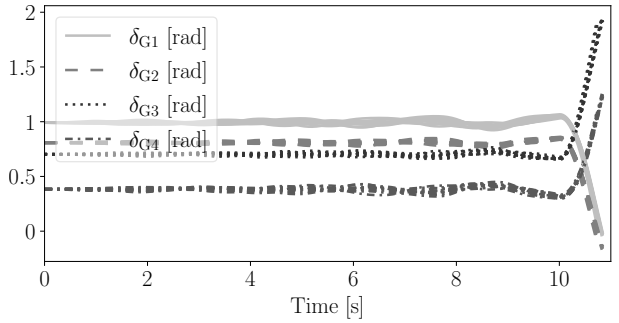

Fig. 9. Rotor angle δ of all the machines of the two-area system for selected unstable trajectories for S2.

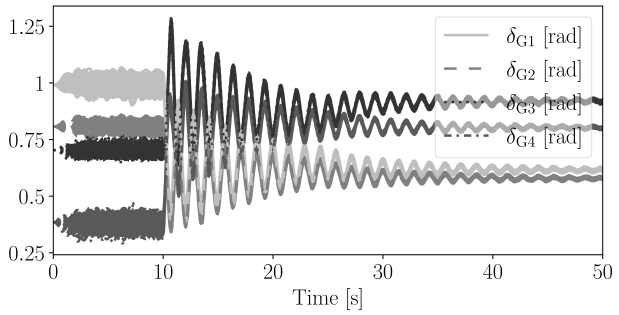

Fig. 10. Rotor angle δ of all the machines of the two-area system for stable trajectories for S3.

correlated volatility on stochastic load consumption, and bus voltage phasors. Stochastic perturbations on wind farms are modeled using the model of correlated wind speeds explained in sub-section IV-C.

The parameters for stochastic load consumption, stochastic bus voltage phasors, and stochastic wind speeds are as follows: $\alpha_p = \alpha_q = \alpha_v = \alpha_\theta = \alpha_w = 1\text{s}^{-1}$, $\sigma_p = 0.5\%$ of p_{L0}, $\sigma_q = 0.5\%$ of q_{L0}, $\sigma_w = 0.5\%$ of w_0, $\sigma_v = 0.3\%$ of v_0 and $\sigma_\theta = 0.3\%$ of θ_0. Note that throughout the case study in this section, the correlation matrix is constructed in such a way that stochastic perturbations on every device connected in same area are correlated whereas no correlation is considered between the devices connected in different areas.

We discuss first the impact of correlated load consumption on σ_{p_g} and σ_{q_g} of the synchronous generators. In this example, wind, and bus voltage phasors do not include noise. Table V shows σ_{p_g} and σ_{q_g} of selected synchronous generators calculated for the three scenarios S1, S2, and S3. The correlation among the stochastic loads has a direct impact on σ_{p_g} and σ_{q_g} of the generators. The value of σ_{p_g} and σ_{q_g} almost doubles when the correlation among stochastic loads is doubled. This is a noteworthy result as the standard deviation of the loads remains the same in all three scenarios. This result also substantiates the results obtained for the two-area system.

Next, we consider the impact of correlated noise on bus voltage phasors on σ_{p_g} and σ_{q_g} of the synchronous generators. In this example, wind, and load power consumption do not include noise. Table VI shows σ_{p_g} and σ_{q_g} of selected synchronous generators calculated for the three scenarios S1, S2, and S3. These results corroborate the results obtained in Table IV. Henceforth, modeling correlation on stochastic bus voltage phasors leads to reduction in the values of σ_{p_g} and σ_{q_g} of the generators. This effect is thus the opposite as the one obtained when varying the correlation of the load power consumption.

In the following example, we model the AIITS incorporating the correlated stochastic perturbations, i.e. correlated stochastic loads, and correlated wind speeds with stochastic perturbations, using the parameter values presented above in this section. To observe the effect of correlation between different stochastic perturbations on the system dynamics, we consider the sum of the trajectories of the relevant quantities such as active power consumption and generation of all the devices connected in the same area. Figure 11 illustrates the sum of the active powers p_{load} consumed by all loads; the sum of the active powers p_{wind} generated by all wind power plants; and the sum of the active powers p_{syn} generated by all synchronous generators for the three scenarios of correlation, i.e. S1, S2, and S3. Despite the fact that the standard deviation of the individual stochastic processes remains the same regardless of the level of correlation being used, Fig. 11 shows that the spread, in terms of standard deviation, of the sum of the quantities above increases as the correlation between the stochastic process is increased.

TABLE V

STANDARD DEVIATION OF ACTIVE AND REACTIVE POWERS OF SYNCHRONOUS GENERATORS FOR THE AIITS WITH CORRELATED STOCHASTIC LOADS

Standard deviation	S1 absolute	S2 % increase	S3 % increase
$\sigma_{p_{g_{\text{HUNT CT}}}}$	0.0025	44	76
$\sigma_{p_{g_{\text{DUBLIN B}}}}$	0.0037	56.76	94.59
$\sigma_{p_{g_{\text{PBEGG4}}}}$	0.0013	53.85	92.31
$\sigma_{p_{g_{\text{PBEGG5}}}}$	0.0012	58.33	100
$\sigma_{p_{g_{\text{PBEGG6}}}}$	0.002	55	90
$\sigma_{q_{g_{\text{HUNT CT}}}}$	0.0004	25	50
$\sigma_{q_{g_{\text{DUBLIN B}}}}$	0.001	50	80
$\sigma_{q_{g_{\text{PBEGG4}}}}$	0.0003	33.33	66.67
$\sigma_{q_{g_{\text{PBEGG5}}}}$	0.0004	50	75
$\sigma_{q_{g_{\text{PBEGG6}}}}$	0.0006	50	83.33

TABLE VI

STANDARD DEVIATION OF ACTIVE AND REACTIVE POWERS OF SYNCHRONOUS GENERATORS FOR THE AIITS WITH CORRELATED STOCHASTIC VOLTAGES

Standard deviation	S1 absolute	S2 % increase	S3 % increase
$\sigma_{p_{g_{\text{HUNT CT}}}}$	0.0193	-22.8	-42.49
$\sigma_{p_{g_{\text{DUBLIN B}}}}$	0.0234	-18.8	-32.48
$\sigma_{p_{g_{\text{PBEGG4}}}}$	0.01	-20	-41
$\sigma_{p_{g_{\text{PBEGG5}}}}$	0.0099	-20.2	-40.4
$\sigma_{p_{g_{\text{PBEGG6}}}}$	0.0127	-18.11	-34.65
$\sigma_{q_{g_{\text{HUNT CT}}}}$	0.0176	-19.89	-50.57
$\sigma_{q_{g_{\text{DUBLIN B}}}}$	0.0298	-18.79	-48.32
$\sigma_{q_{g_{\text{PBEGG4}}}}$	0.0159	-22.64	-49.06
$\sigma_{q_{g_{\text{PBEGG5}}}}$	0.0148	-20.27	-41.89
$\sigma_{q_{g_{\text{PBEGG6}}}}$	0.0188	-16.49	-40.43

Finally, we consider a model of the AIITS that incorporates all stochastic perturbations, i.e. correlated stochastic loads, correlated stochastic bus voltage phasors, and correlated wind speeds with stochastic perturbations, using the parameter values presented above in this section. In addition to the stochastic perturbations, the AIITS undergoes a disconnection of a load connected to East-West interconnector at $t = 10$ s.

Figure 12 shows the time domain profile of voltage magnitude at bus Woodland, for the 1,000 simulations, for S1, i.e. for the fully uncorrelated SDAE model. The black solid line shows the mean value of the 1,000 trajectories, which reflects the voltage profile of a deterministic solution, since all Wiener processes have zero average. This is evident from Fig. 12 that the mean trajectory coincides with the deterministic trajectory. The deterministic trajectory is obtained for simulating AIITS for same fault conditions without including the stochastic processes. Figure 12 indicates that the voltage profile for the deterministic solution is below the maximum voltage limit, which is shown by a dashed line. It is also relevant to note that 24.4% of the trajectories exceed the maximum voltage limit at least once in the period 10 s $< t < 30$ s. This result can be relevant for TSOs as grid codes do not allow voltage variations above or below 10%. Moreover overvoltage protections are implemented in some systems and these protections can be triggered if voltage limits are violated in transient conditions.

Figures 13 and 14 illustrate the 1,000 trajectories of voltage magnitude at bus Woodland, for S2 and S3, respectively. Results indicate that the higher the correlation among the processes the lower the standard deviation of the trajectories. For S3, i.e. for the maximum correlation considered in this case study, no trajectory crosses the maximum voltage limit. These results are summarized in Table VII. In this example, the uncorrelated stochastic model shows more conservative results than the scenarios that take into account correlation.

The examples discussed in the case study lead to conclude that the correlation among stochastic processes has a relevant impact on the dynamic response of the system and that such an impact is not known *a priori* as, in some cases, taking into account correlation leads to more conservative results and in

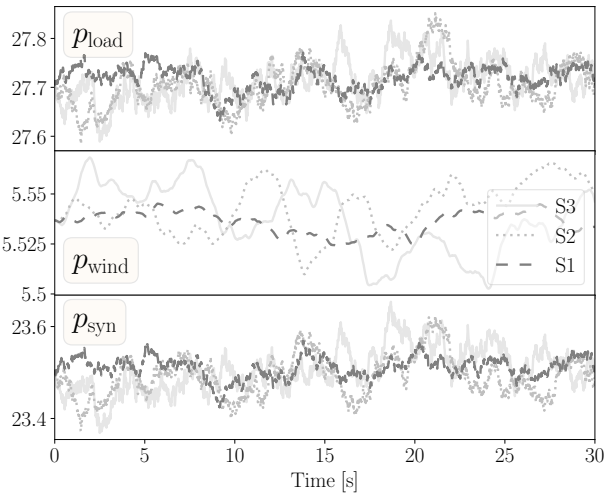

Fig. 11. Total active power load consumption (p_{load}); total active power generation (p_{wind}) by wind power plants; and total active power generation (p_{syn}) by conventional power plants for the three scenarios of correlation, i.e. S1, S2, and S3. All the values are in [pu], with a base of 100 MVA.

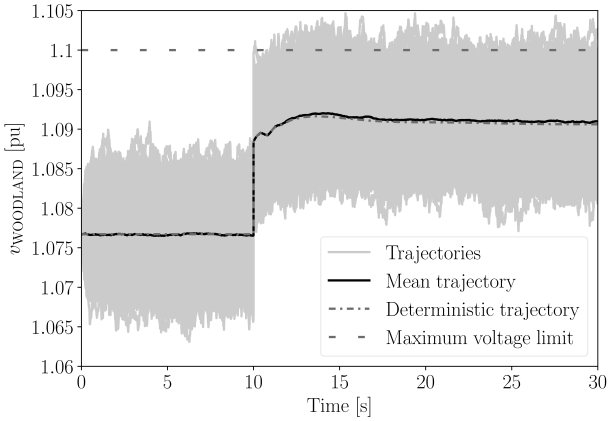

Fig. 12. Bus voltage magnitude at bus Woodland for S1.

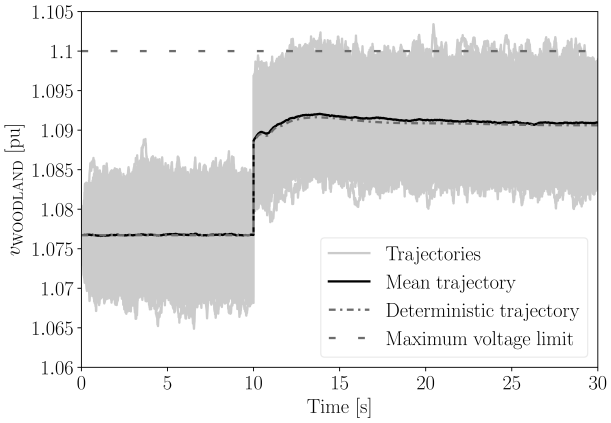

Fig. 13. Bus voltage magnitude at bus Woodland for S2.

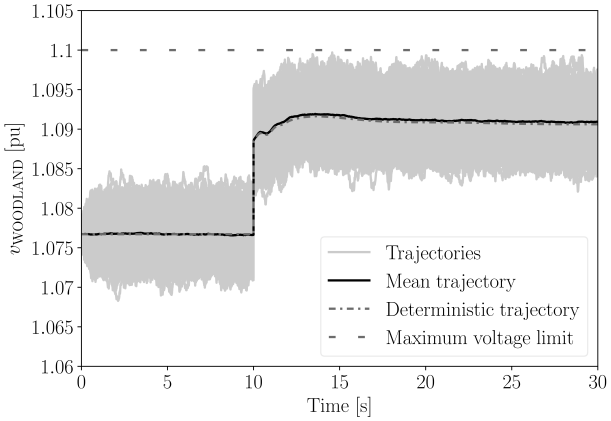

Fig. 14. Bus voltage magnitude at bus Woodland for S3.

TABLE VII
TRAJECTORIES WITH OVER-VOLTAGES FOR THE AIITS

Scenarios	Trajectories with over-voltages
S1	244 (24.4%)
S2	70 (7%)
S3	0

others to less conservative results than assuming fully uncorrelated processes. Correlation has thus to be modeled correctly to properly estimate the standard deviation of variables and the stability of the system.

As a final remark, we note that the the noise included in conventional generators, wind power plants and loads in this case study lead to relatively small peak-to-peak power variations, of the order of 1 MW. Nevertheless, such varitions have a non-negligible effect on the dynamic response of the whole system. It is important to note that it is not the power variation of the single wind power plant or load that is relevant but, rather, how such a variation is correlated to the variations of the other wind power plants. It is the combined effect that can make a difference in the transient behavior fo the system.

VII. Conclusions and Future Works

This paper presents a general approach to model power systems as a set of correlated SDAEs. The generality and scalability of the proposed model is demonstrated through simulations based on detailed dynamic model of the all-island Irish transmission system. Simulation results indicate that correlation plays a significant role in the dynamic response of the system as it can modify the standard deviation of the trajectories. Moreover, the case study demonstrated that a power system deemed to be stable, in the presence of uncorrelated noise, may become unstable due to the presence of correlated noise, despite the fact that the stochastic processes have same statistical properties in both cases. A precise estimation of the correlations among the stochastic processes appears thus an important parameter to be defined by system operators for the transient stability analysis of the grid.

Various future works can be devised. As said above, the proper estimation of the actual values of correlations among the physical stochastic processes is a relevant step that can help set-up and maybe improve the proposed model. This of course requires a large amount of measurement data. At the time of writing this paper, however, it is very difficult to obtain measurement data that can be actually utilized to calculating the correlation matrix for a real-world system. The data made available to us by TSOs, in fact, are either detailed but spanning short periods, i.e., considering only specific events (and thus not allowing calculating correlation matrix) or large time series but consisting of values averaged over several minutes, e.g., 15 minutes (and thus inadequate for short-term dynamic analysis). It is our understanding that TSOs have access to such detailed data through SCADA systems, as mentioned in the websites, but is not being stored in such a detail because it requires large amount of storage and until now it was not required by a modeling scheme such as the one introduced in this paper.

The results discussed in this work highlight the importance of modeling correlated stochastic processes in power systems. The technology to gather and store such a large amount of information is already available and it can be used for the evaluation of statical properties so that they can be utilized to model accurately correlated processes for dynamic analysis. Another important aspect that can be deduced from data is whether the correlation among processes is constant or variable with time. This can lead to various scenarios. Finally, we anticipate that the correlation of stochastic processes depends on the time scale considered, e.g. short term or long-term dynamics. This appears another relevant topic to future work.

References

[1] K. Wang and M. L. Crow, "Numerical simulation of stochastic differential algebraic equations for power system transient stability with random loads," in *IEEE PES General Meeting*, San Diego, CA, USA, Jul. 2011.

[2] Z. Y. Dong, J. H. Zhao, and D. J. Hill, "Numerical Simulation for Stochastic Transient Stability Assessment," *IEEE Transactions on Power Systems*, vol. 27, no. 4, pp. 1741–1749, Nov. 2012.

[3] F. Milano and R. Zárate-Miñano, "A systematic method to model power systems as stochastic differential algebraic equations," *IEEE Transactions on Power Systems*, vol. 28, no. 4, pp. 4537–4544, Nov 2013.

[4] A. J. Conejo, M. Carrión, and J. M. Morales, *Decision Making Under Uncertainty in Electricity Markets*. New York, NY: Springer, 2010.

[5] C. M. Roberts, E. M. Stewart, and F. Milano, "Validation of the ornstein-uhlenbeck process for load modeling based on μPMU measurements," in *Power System Computation Conference (PSCC)*, Genova, Italy, 2016.

[6] S. Aboreshaid, R. Billinton, and M. Fotuhi-Firuzabad, "Probabilistic transient stability studies using the method of bisection [power systems]," *IEEE Transactions on Power Systems*, vol. 11, no. 4, pp. 1990–1995, Nov. 1996.

[7] R. N. Allan, R. Billinton, A. M. Breipohl, and C. H. Grigg, "Bibliography on the application of probability methods in power system reliability evaluation: 1987-1991," *IEEE Transactions on Power Systems*, vol. 9, no. 1, pp. 41–49, Feb. 1994.

[8] R. Billinton, M. Fotuhi-Firuzabad, and L. Bertling, "Bibliography on the application of probability methods in power system reliability evaluation 1996-1999," *IEEE Transactions on Power Systems*, vol. 16, no. 4, pp. 595–602, Nov. 2001.

[9] X. Li, X. Zhang, L. Wu, P. Lu, and S. Zhang, "Transmission line overload risk assessment for power systems with wind and load-power generation correlation," *IEEE Transactions on Smart Grid*, vol. 6, no. 3, pp. 1233–1242, 2015.

[10] S. Tao, Y. Li, X. Xiao, and L. Yao, "Load forecasting based on short-term correlation clustering," in *2017 IEEE Innovative Smart Grid Technologies - Asia (ISGT-Asia)*, 2017, pp. 1–7.

[11] S. Peng, J. Tang, and W. Li, "Probabilistic power flow for ac/vsc-mtdc hybrid grids considering rank correlation among diverse uncertainty sources," *IEEE Transactions on Power Systems*, vol. 32, no. 5, pp. 4035–4044, 2017.

[12] X. Liu, Z. Zhang, W. Wang, H. Zheng, J. Hao, and Y. Chen, "Two-stage robust optimal dispatch method considering wind power and load correlation," in *2018 2nd IEEE Conference on Energy Internet and Energy System Integration (EI2)*, 2018, pp. 1–6.

[13] X. Mi, J. Wang, and R. Wang, "Stochastic small disturbance stability analysis of nonlinear multi-machine system with ito differential equation," *International Journal of Electrical Power and Energy Systems*, vol. 101, pp. 439 – 457, 2018.

[14] X. Yan, W. Fushuan, Z. Hongwei, C. Minghui, Y. Zeng, and S. Huiyu, "Stochastic small signal stability of a power system with uncertainties," *Energies*, vol. 11, no. 11, p. 2980, Nov 2018.

[15] P. Ju, H. Li, C. Gan, Y. Liu, Y. Yu, and Y. Liu, "Analytical assessment for transient stability under stochastic continuous disturbances," *IEEE Transactions on Power Systems*, vol. 33, no. 2, pp. 2004–2014, March 2018.

[16] P. Vorobev, D. M. Greenwood, J. H. Bell, J. W. Bialek, P. C. Taylor, and K. Turitsyn, "Deadbands, droop, and inertia impact on power system frequency distribution," *IEEE Transactions on Power Systems*, vol. 34, no. 4, pp. 3098–3108, 2019.

[17] G. M. Jónsdóttir and F. Milano, "Modeling correlation of active and reactive power of loads for short-term analysis of power systems," in *20th International Conference on Environmental and Electrical Engineering (EEEIC)*, Madrid, Spain, 2020, pp. 1 – 5.

[18] E. Kloeden and E. Platen, *Numerical Solution of Stochastic Differential Equations*. New York, NY, third edition: Springer, 1999.

[19] F. Milano, *Power System Modelling and Scripting*. London: Springer, 2010.

[20] E. Kloeden, E. Platen, and H. Schurz, *Numerical Solution of SDE Through Computer Experiments*. New York, NY, third edition: Springer, 2003.
[21] P. E. Protter, *Stochastic Integration and Differential Equations*. New York, NY, second edition: Springer, 2004.
[22] M. Kendall and A. Stuart, *The advanced theory of statistics. Vol.2: Inference and relationship*, 4th ed. London, UK: Griffin, 1979.
[23] S. Dipple, A. Choudhary, J. Flamino, B. K., Szymanski, and G. Korniss, "Using correlated stochastic differential equations to forecast cryptocurrency rates and social media activities," *Applied Network Science*, vol. 5, no. 17, 2020.
[24] C. O. Nwankpa and S. M. Shahidehpour, "Stochastic model for power system planning studies," *IEE Proceedings-C*, vol. 138, no. 4, pp. 307–320, Jul. 1991.
[25] R. Zárate-Miñano, F. M. Mele, and F. Milano, "Sde-based wind speed models with weibull distribution and exponential autocorrelation," in *2016 IEEE Power and Energy Society General Meeting (PESGM)*, 2016, pp. 1–5.
[26] R. Zárate-Miñano and F. Milano, "Construction of sde-based wind speed models with exponentially decaying autocorrelation," *Renewable Energy*, vol. 94, pp. 186 – 196, 2016.
[27] X. Chen, J. Lin, F. Liu, and Y. Song, "Stochastic assessment of agc systems under non-gaussian uncertainty," *IEEE Transactions on Power Systems*, vol. 34, no. 1, pp. 705–717, 2019.
[28] M. Perninge, M. Amelin, and V. Knazkins, "Load modeling using the ornstein-uhlenbeck process," in *2008 IEEE 2nd International Power and Energy Conference*, 2008, pp. 819–821.
[29] H. Hua, Y. Qin, C. Hao, and J. Cao, "Stochastic optimal control for energy internet: A bottom-up energy management approach," *IEEE Transactions on Industrial Informatics*, vol. 15, no. 3, pp. 1788–1797, 2019.
[30] M. Olsson, M. Perninge, and L. Söder, "Modeling real-time balancing power demands in wind power systems using stochastic differential equations," *Electric Power System Research*, vol. 80, no. 8, pp. 966–974, Aug. 2010.
[31] A. Loukatou, S. Howell, P. Johnson, and P. Duck, "Stochastic wind speed modelling for estimation of expected wind power output," *Applied Energy*, vol. 228, pp. 1328 – 1340, 2018.
[32] F. E. Benth, L. Di Persio, and S. Lavagnini, "Stochastic modeling of wind derivatives in energy markets," *Risks*, vol. 6, no. 2, 2018.
[33] G. M. Jónsdóttir and F. Milano, "Data-based continuous wind speed models with arbitrary probability distribution and autocorrelation," *Renewable Energy*, vol. 143, pp. 368 – 376, 2019.
[34] F. M. Mele, R. Zárate-Miñano, and F. Milano, "Modeling load stochastic jumps for power systems dynamic analysis," *IEEE Transactions on Power Systems*, vol. 34, no. 6, pp. 5087–5090, 2019.
[35] P. Kundur, *Power System Stability and Control*. New York: Mc-Grall Hill, 1994.

Muhammad Adeen (S'20) received B.E. electrical engineering degree from National University of Sciences and Technology, Pakistan in 2013 and M.Sc. degree in electrical engineering from Politecnico di Milano, Italy in 2017. Since May 2018, he is a Ph.D. candidate with the Department of Electrical Engineering in Univ. College Dublin, Ireland. His current research interests include stochastic processes, power system modeling and dynamic analysis.

Federico Milano (F'16) received from the Univ. of Genoa, Italy, the ME and Ph.D. in Electrical Eng. in 1999 and 2003, respectively. From 2001 to 2002 he was with the Univ. of Waterloo, Canada, as a Visiting Scholar. From 2003 to 2013, he was with the Univ. of Castilla-La Mancha, Spain. In 2013, he joined the Univ. College Dublin, Ireland, where he is currently Prof. of Power Systems Control and Protections and Head of Elec. Eng. His research interests include power system modeling, control and stability analysis.